
Princeton Plasma Physics Laboratory

PPPL-

PPPL-



Prepared for the U.S. Department of Energy under Contract DE-AC02-09CH11466.

Princeton Plasma Physics Laboratory

Report Disclaimers

Full Legal Disclaimer

This report was prepared as an account of work sponsored by an agency of the United States Government. Neither the United States Government nor any agency thereof, nor any of their employees, nor any of their contractors, subcontractors or their employees, makes any warranty, express or implied, or assumes any legal liability or responsibility for the accuracy, completeness, or any third party's use or the results of such use of any information, apparatus, product, or process disclosed, or represents that its use would not infringe privately owned rights. Reference herein to any specific commercial product, process, or service by trade name, trademark, manufacturer, or otherwise, does not necessarily constitute or imply its endorsement, recommendation, or favoring by the United States Government or any agency thereof or its contractors or subcontractors. The views and opinions of authors expressed herein do not necessarily state or reflect those of the United States Government or any agency thereof.

Trademark Disclaimer

Reference herein to any specific commercial product, process, or service by trade name, trademark, manufacturer, or otherwise, does not necessarily constitute or imply its endorsement, recommendation, or favoring by the United States Government or any agency thereof or its contractors or subcontractors.

PPPL Report Availability

Princeton Plasma Physics Laboratory:

<http://www.pppl.gov/techreports.cfm>

Office of Scientific and Technical Information (OSTI):

<http://www.osti.gov/bridge>

Related Links:

[U.S. Department of Energy](#)

[Office of Scientific and Technical Information](#)

[Fusion Links](#)

Observation of non-Maxwellian electron distributions in the NSTX divertor

M. A. Jaworski^{a,*}, M.G. Bell^a, T.K. Gray^b, R. Kaita^a, I. Kaganovich^a, J. Kallman^a, H.W. Kugel^a, B. LeBlanc^a, A.G. McLean^c, S.A. Sabbagh^d, F. Scotti^a, V.A. Soukhanovskii^c, and D.P. Stotler^a

^a Princeton Plasma Physics Laboratory, Princeton, NJ, 08543, USA

^b Oak Ridge National Laboratory, Oak Ridge, TN 37831, USA

^c Lawrence Livermore National Laboratory, Livermore, CA 94551, USA

^d Columbia University, New York, NY 10027, USA

Abstract

The scrape-off layer plasma at the tokamak region is characterized by open field lines and often contains large variations in plasma properties along these field-lines. Proper characterization of local plasma conditions is critical to assessing plasma-material interaction processes occurring at the target. Langmuir probes are frequently employed in tokamak divertors but are challenging to interpretation. A kinetic interpretation for Langmuir probes in NSTX has yielded non-Maxwellian electron distributions in the divertor characterized by cool bulk populations and energetic tail populations with temperatures of 2–4 times the bulk. Spectroscopic analysis and modeling confirms the bulk plasma temperature and density which can only be obtained with the kinetic interpretation.

PACS: 52.25.Fi, 52.25.Xz, 52.40.Hf, 52.55.Rk, 52.70.Nc

JNM Keywords: Magnetic fusion energy, edge plasma diagnosis

PSI-20 Keywords: divertor, electron parallel transport, Langmuir probes, kinetic effects

**Corresponding author address:* USA

**Corresponding author email:* mjaworsk@pppl.gov

Presenting author: Michael A. Jaworski

Presenting author e-mail: mjaworsk@pppl.gov

1 Introduction

Langmuir probes are notoriously difficult to interpret[1]. Probe theory is well developed for low density, low temperature, unmagnetized discharge plasmas[2]. Systems can be constructed or even purchased with the capability of measuring electron distribution functions to a high-degree of accuracy. In tokamak devices, however, comparison of Langmuir probe measurements with other diagnostics often indicate inconsistencies. The ASDEX machine compared divertor Langmuir probe measurements with laser scattering diagnostics where it was found that the probe temperatures exceeded laser scattering by a factor of ≈ 2 [3]. Similar comparison was made in DIII-D with the Divertor Thomson System (DTS) where Langmuir probe measurements were found to exceed the temperatures found by the DTS for the low-density conditions present in this experiment[4]. In comparison with infrared thermography, calculated sheath heat transmission coefficients are often found to be at odds with fluid theory[5]. It has been hypothesized that energetic tail populations could explain many observations of this type[6].

In simulating edge plasmas, Chodura showed that inclusion of recycling particles resulted in non-Maxwellian distributions at the target plate[7]. Batishchev also found energetic tail populations in both attached and detached plasma simulations[8]. Electrons were simulated on a fluid background by Aho-Mantila using the ASCOT code again finding non-Maxwellian distributions at the target[9]. The impact of non-Maxwellian electron distributions on diagnostic interpretation is also an active area of research[10, 11].

Recent developments in probe theory now give the possibility of experimentally verifying the distribution functions in the tokamak divertor. A kinetic probe interpretation has been developed on gas discharge devices[2] and has recently been extended to tokamaks (first on CASTOR[12] and recently on NSTX[13]). This paper briefly reviews the criteria for fluid assumptions to remain valid and the kinetic probe interpretation method. We then compare the obtained plasma parameters to spectroscopic observations to assess the validity of the kinetic interpretation.

2 Theory

The issue of the appropriate scale length can be simply illustrated by considering the equations describing the electron temperature in a scrape-off layer(SOL). In the case of conduction-limited heat transport in the absence of energy sources, the electron heat flux is given by the following $q_{\parallel} = -\kappa_0 T^{5/2} \partial T / \partial x$ [14]. Here q_{\parallel} is the amount of power conducted in the direction of the field line, x . An important parameter is the temperature scale length, L_{Te} along the flux tube which can be calculated as:

$$L_{Te} = \frac{T}{\nabla T} = \frac{\kappa_0 T^{7/2}}{q_{\parallel}} \quad (1)$$

illustrating that as the plasma temperature decreases approaching a divertor target, that for constant conducted power, the temperature-gradient scale-length also decreases with temperature. Figure 1 shows just such a temperature and scale-length profile for typical NSTX parameters of 50 MW/m² parallel heatflux and a target temperature of 4 eV.

[Figure 1 about here.]

The strong reduction of the temperature-gradient scale-length was considered by Chodura and is now reviewed[7]. Collisionality is typically defined as a ratio of scale lengths, one of which being the self-collision mean-free-path such that $\nu_{SOL}^* = L/\lambda_{ee}$ [14]. Here λ_{ee} is the mean-free-path for self-collisions and L is a characteristic scale length of the system. Historically, the entire SOL has been reduced to a single collisionality calculated for mid-plane parameters[14] with the approximation of $\nu_{SOL}^* \approx 10^{-16} n_u L / T_u^2$ used with temperature in eV, density in m⁻³ and the flux-tube connection length in m used for the value of L . Chodura considered the fluid description and showed that the heat-carrying electrons have energies of 3–5 T_e . These electrons must be collisional enough to thermalize creating the criteria that the collisionality of the thermal electrons must be of order 100 or greater for fluid theory to be valid. In addition, it was pointed out that *the relevant scale length in such instances is the temperature scale length of the plasma, not necessarily, the connection length of the flux tube*. Figure 1 also shows the electron-electron mean-free-path for the heat-carrying electrons for comparison with the temperature-gradient scale-length. One can see that in the conduction-limited regime the

mean-free-path of these electrons exceed the gradient scale-length near the target plate. Rearranging the eq. 1 and the definition for collisionality one finds an approximate scaling for the temperature above which the fluid description is valid as (*c.f.* eq. 2.11 of [7]):

$$T_e^{3/2} \gtrsim \frac{10^{18} q_{\parallel}}{\kappa_0 n_e} \quad (2)$$

For typical NSTX conditions found in this study of 50 MW/m^2 parallel heat flux and target densities of $3.5 \times 10^{20} \text{ m}^{-3}$, one finds that the minimum temperature at the target is about 15 eV.

The Langmuir probe theory and methodology has been discussed at length in previous works[12, 13]. In terms of scale length, when the probe perturbation scale is much smaller than the energy scale-length of the local plasma, then the kinetic interpretation may be applied. In these cases the kinetic equations can be manipulated to give the approximate distribution function as[12]:

$$f(\epsilon) \propto (U)^{-3/2} \frac{dI}{dU} \quad (3)$$

where $f(\epsilon)$ is the distribution function as a function of energy, U is the voltage and I is the current from the probe.

The numerical method used for this study rely on taking the first derivative of the I-V characteristic. Alternative techniques using integral methods may be applicable but are not considered here[15, 16]. In NSTX, the degree of turbulence can reduce the quality of data (defined through moments of the time-series signals). We concentrate on applying the method near the strike-point where fluctuating quantities vary by less than 10% (defined by the ratio of the signal R.M.S. to the mean) as monitored by nearby triple Langmuir probes[17]. When the fluctuation level of the plasma is less than 10% and the skewness and kurtosis indicate Gaussian probability distribution functions, then the analysis is carried forward. It is known that sheath-growth can produce spurious tail populations in distribution functions derived from probe data[2]. In the thin-sheath regime (the entire data set for this study), the expected onset voltage where the expanding sheath would affect the first derivative of the I-V characteristic is calculated using the Child-Langmuir relations[18] and data from this region are excluded from temperature fits. Details of the probe theory and analysis methodology are reported in ref. [13].

The OEDGE code suite is used for empirical plasma reconstruction of the available diagnostics[19]. Neutral hydrogen is modeled using the EIRENE code[20].

A collisional-radiative model is used to determine excited state populations for given plasma density, neutral density and temperatures[21]. The CollRad code[21] is used to evaluate high- n Balmer line-brightnesses from the divertor plasmas of interest here. Emission rates for each line is then calculated from available transition probabilities[22].

3 Experimental Setup and Results

NSTX is a medium-size, spherical tokamak with major radius of 0.9 m and aspect ratio as low as 1.2[23]. Typical toroidal field strength is 0.45 T and 0.8 MA plasma current. Plasma discharges typically last about 1 s, with heating power largely supplied by neutral beam injection with 4 MW input.

Figure 2 shows parameters of the discharge which will be considered in detail. The period of time from 400–800 ms shows the region defined as “flat-top” where the plasma is in a stationary state in terms of current and input power. Strike-point control is used to maintain a given radial position for the outer strike point. Natural variation in the discharge prevents perfect operation of the controller and some variability is observed. The strike-point region is characterized by large local gradients and the variability in the example Langmuir probe I_{sat} signal is a result this motion. The probe-voltage sweep-rate of 500 Hz creates a complete I-V characteristic every 1 ms; much faster than the motion of the strike-point. This allows a single probe to cover a significant distance with respect to the nominal strike-point position as reported by equilibrium reconstructions.

NSTX performs regular wall-conditioning with the usage of evaporated lithium coatings. The majority of plasma-facing components (PFCs) in the NSTX device consist of Union-Carbide type “ATJ” graphite. In the lower divertor of NSTX, the liquid lithium divertor (LLD) was installed for further studies of high-Z components with lithium coatings in the solid and liquid state[24]. Discharges under consideration operated with the outer strike-point impinging the LLD. The high-density Langmuir probe array used for this study is located in-between one of the four LLD plate segments.

[Figure 2 about here.]

The kinetic interpretation of the I-V characteristics yield the following values for this discharge: the plasmas can be characterized by a bi-modal distribution (*i.e.* two-temperature distribution): a cool bulk plasma in the range of 3–5 eV and a higher energy tail population in the range of 10–25 eV. An example distribution for a single probe is shown in fig. 3. The density at the sheath-edge of the local plasma is determined by the following:

$$n_{se} = \frac{I_{sat}^+}{e\bar{c}_s A_{eff}} \quad (4)$$

where \bar{c}_s is the ion sound speed, A_{eff} is the probe collection area and e is the electronic charge. The dependence on temperature via the ion sound-speed provides a separation between the classical probe method and kinetic probe interpretations.

To make a comparison between diagnostics, a large number of observations are collected and compiled into a target-plate profile. The set of I-V analyses are averaged to provide a “best estimate” for the type of plasma that would be viewed by a spectrometer for the integration times of the diagnostic and the spatial extent of the viewing chord. The average bulk temperature obtained from the kinetic interpretation from this set of probe observations is 3.4 eV whereas the classical interpretation yields 8.3 eV as an average. Densities are $2.5 \times 10^{20} \text{ m}^{-3}$ and $1.6 \times 10^{20} \text{ m}^{-3}$ for the kinetic and classical interpretations respectively.

[Figure 3 about here.]

An example spectrum from the NSTX spectroscopy system[25] is shown in figure 4. The presence of high- n Balmer lines is indicative of significant recombination — a low temperature plasma process. Quantitatively, the density can be deduced from the amount of broadening of each of the spectral lines. Voigt line profiles were fitted to each of the B6-B9 lines taking into account instrumental functions and thermal broadening to obtain the Stark component as was done in ref. [26]. The densities derived from each of the lines were averaged together to provide a single density of $3.6 \pm 1.5 \times 10^{20} \text{ m}^{-3}$. A total line brightness is computed by numerical integration of the data in a narrow band about each line.

[Figure 4 about here.]

Both kinetic and classical probe interpretations were used in OEDGE plasma reconstructions. For these reconstructions the full density and temperature profile available from the Langmuir probes is used. The neutral solution from EIRENE for one set of density and temperature varies from peak values of about $8.2 \times 10^{18} \text{ m}^{-3}$ with the classical probe values to $2.7 \times 10^{19} \text{ m}^{-3}$ with the kinetic probe analysis. The ratio of neutrals to ions varies in these two cases from 0.08–0.13. We set the ratio to a constant 0.1 for convenience (using a varying ratio in the following analysis does not significantly alter the results). The CR-model is used to determine the species populations using these ion and neutral quantities and the respective plasma conditions. With the code, the temperature is scanned from 2–15 eV. The result of the analysis is a set of line-brightnesses for each temperature condition. For comparison, the lines are normalized to the brightest line available ($\approx 410 \text{ nm}$) to illustrate the change in spectra and shown in figure 5. The observed ratios from the spectrometer can be bound between 3–5 eV from the CR-modeling.

[Figure 5 about here.]

Table 1 shows a summary of observations comparing the probe interpretations and results from spectroscopic analysis.

[Table 1 about here.]

4 Discussion and Conclusions

One sees that better agreement between independent diagnostics is found with the kinetic probe interpretation. The very existence of the high- n Balmer lines suggests the presence of a low temperature plasma and this is confirmed by the CR modeling results. The spectroscopic broadening result for density is only weakly dependent on electron temperature providing a robust result as the temperature itself is in question. The spectroscopic results and modeling essentially confirm the validity of the kinetic interpretation showing a cool bulk population.

The local temperature, even using the classical method, is below what one would expect as valid for the fluid conduction model ($\approx 4 \text{ eV}$ vs. 15 eV) and therefore violates the Chodura

criteria that was restated as eq. 2. Although this result may be counter-intuitive considering the high density and low temperatures present at the target plate, nevertheless one must consider kinetic transport effects in such conditions.

This result could have significant impact on projections to ITER as it is essential to reduce the temperatures at the target plates to eliminate erosion by sputtering. This reduction in temperature toward the target *is precisely where kinetic effects will occur*. This effect was already shown in modeling by Batishchev[8], and this work provides experimental evidence that these kinetic effects do, indeed, occur. Earlier work showed, however, that the plasma-to-floating potential difference is most strongly correlated with the amount of energy in the higher-temperature electron population[13]. This indicates that despite the reduction to low bulk temperatures, a tail population could create an elevated sheath potential leading to larger than expected sputtering yields.

Studies of non-local electron transport effects have begun through the use of analytics and numerical simulations. Non-local transport occurs when high-energy electrons pass to different regions of the plasma due to the decrease in collision cross-section with increasing energy. A velocity-dependent Krook model[27] has been applied using the OEDGE background plasma as an initial condition. Comparison of the derived distribution functions using the velocity-dependent Krook model reproduce a tail population with the correct temperatures as observed in the probe results (details are left to a future publication).

In summary: non-Maxwellian electron energy distributions have been observed in the NSTX divertor. These observations have been obtained through the use of a kinetic probe interpretation method. OEDGE interpretive modeling has been applied to reconstruct the local plasma and neutral solutions to aid spectroscopic interpretation. The characteristics of the bulk plasma are confirmed with a combination of spectroscopic analysis and collisional-radiative modeling. The existence of kinetic effects should not be unexpected considering these plasma conditions violate the fluid-model criteria set forth by Chodura for conduction-limited electron transport. Initial studies with analytics using the OEDGE fluid background as an initial condition have also shown the generation of tail populations suggesting non-local electron transport could be the root cause of the non-Maxwellian distributions, consistent with earlier simulations and the-

oretical works.

Acknowledgments

The authors wish to thank the reviewers for comments that have generally improve the quality of this manuscript. This work is supported under the U.S. Department of Energy contract #DE-AC02-09CHI1466.

References

- [1] G. Matthews, *Plasma Phys. Control. Fusion* 36 (1994) 1595–1628.
- [2] V. Godyak, V. Demidov, *J. Phys. D: Appl. Phys.* 44 (2011) 233001.
- [3] G. Fussman, *et al.*, *J. Nucl. Mater.* 128–129 (1984) 350–358.
- [4] J. Watkins, *et al.*, *J. Nucl. Mater.* 290–293 (2001) 778–782.
- [5] J. Marki, *et al.*, *J. Nucl. Mater.* 363–365 (2007) 382–388.
- [6] P. Stangeby, *Plasma Phys. Control. Fusion* 37 (1995) 1031–1037.
- [7] R. Chodura, *Contrib. Plasma Phys.* 32 (1992) 219–230.
- [8] O. Batishchev, *et al.*, *Phys. Plasmas* 4 (1997) 1672–1680.
- [9] L. Aho-Mantila, *et al.*, *Plasma Phys. Control. Fusion* 50 (2008) 065021.
- [10] D. Tskhakaya, *et al.*, *J. Nucl. Mater.* 415 (2011) S860.
- [11] J. Gunn, *et al.*, *Phys. Plasmas* 14 (2007) 032501.
- [12] T. Popov, *et al.*, *Plasma Phys. Control. Fusion* 51 (2009) 065014.
- [13] M. Jaworski, *et al.*, *Fusion Eng. Des.* 87 (2012) 1711–1718.
- [14] P. C. Stangeby, *The Plasma Boundary of Magnetic Fusion Devices*, Institute of Physics Publishing, Philadelphia, PA, 2000.

- [15] M. Kocan, *et al.*, Measurements of the parallel ion velocity distribution at the plasma-sheath interface, *J. Nucl. Mater. these proceedings*.
- [16] A. El Saghir, *et al.*, *IEEE Trans. Plasma Sci.* 38 (2010) 156–162.
- [17] M. Jaworski, *et al.*, *Rev. Sci. Instrum.* 81 (2010) 10E130.
- [18] J. Gunn, *et al.*, *Rev. Sci. Instrum.* 68 (1997) 404–407.
- [19] P. Stangeby, *et al.*, *J. Nucl. Mater.* 313–316 (2003) 883–887.
- [20] D. Reiter, *J. Nucl. Mater.* 196–198 (1992) 80–89.
- [21] D. Stotler, *et al.*, User’s guide for DEGAS 2 release v. 4.3, Tech. rep., Princeton Plasma Physics Laboratory (2009).
- [22] Y. Ralchenko, A. Kramida, NIST ASD Team, NIST atomic spectra database, Online, National Institute of Standards and Technology, available: <http://physics.nist.gov/asd> (2011).
- [23] M. Ono, *et al.*, *Nucl. Fusion* 40 (2000) 557–561.
- [24] H. Kugel, *et al.*, *Fusion Eng. Des.* 84 (2009) 1125–1129.
- [25] V. Soukhanovskii, *et al.*, *Rev. Sci. Instrum.* 77 (2006) 10F127.
- [26] F. Scotti, *et al.*, *J. Nucl. Mater.* 415 (2011) S405–S408.
- [27] W. Mannheimer, D. Colombant, V. Goncharov, *Phys. Plasma* 15 (2008) 083103.

List of Figures

1	Plot showing temperature and the temperature-gradient scale-length as a function of distance from the PFC surface for a conduction limited SOL profile. The target plasma is 4 eV at $4e20 \text{ m}^{-3}$ which yields $\approx 4 \text{ MW/m}^2$ at 5° angle of incidence, similar to divertor plasmas measured in this study. The red band indicates the electron-electron mean-free-path for electrons with mean energy of $3-5T_e$	12
2	Discharge waveforms during NSTX operations showing plasma current, heating power, outer strike-point position and an example Langmuir probe I_{sat} signal (probe located at $R=0.71\text{cm}$). Radial extents of the full probe array are shown in (c).	13
3	Plot showing derived electron velocity distribution function(EVDF) vs. energy. EVDF derived using kinetic interpretation of the I-V characteristic with best-fit values of a bi-modal distribution also shown. Electron temperature derived from conventional analysis of the I-V characteristic yields 13 eV.	14
4	Plot of divertor emission between 370–415 nm located over the probe array used in this study. The Hydrogen Balmer lines 6–11 have been labeled.	15
5	Plot of relative line intensities vs. wavelength for 10% neutral background density and a range of electron temperatures of the background plasma. All line intensities normalized to the Balmer-6 line at 410 nm. Region between 3–5 eV highlighted to indicate range of temperatures bounding experimental data.	16

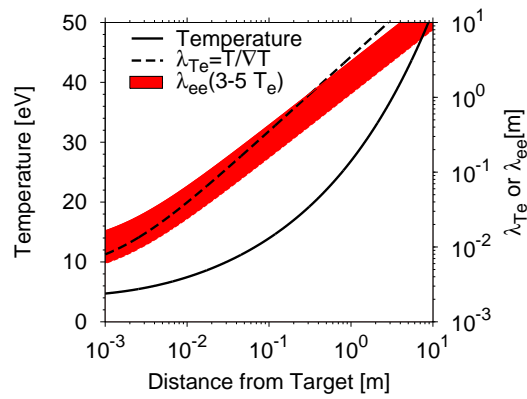


Figure 1: Plot showing temperature and the temperature-gradient scale-length as a function of distance from the PFC surface for a conduction limited SOL profile. The target plasma is 4 eV at $4e20 \text{ m}^{-3}$ which yields $\approx 4 \text{ MW/m}^2$ at 5° angle of incidence, similar to divertor plasmas measured in this study. The red band indicates the electron-electron mean-free-path for electrons with mean energy of $3-5T_e$.

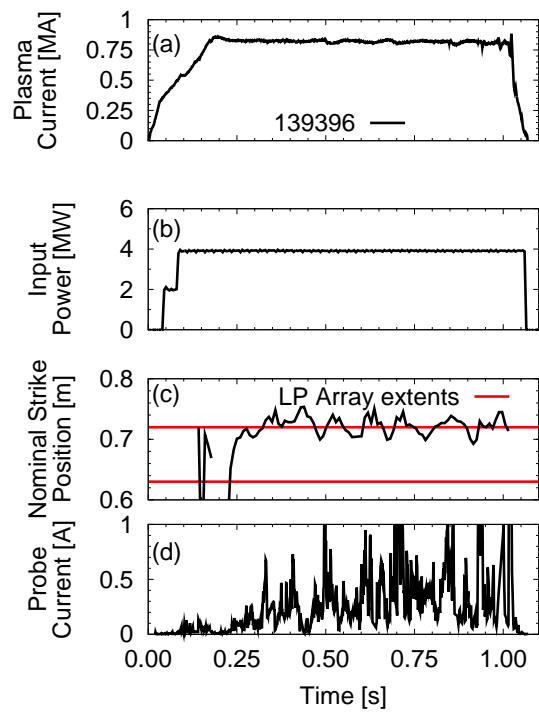


Figure 2: Discharge waveforms during NSTX operations showing plasma current, heating power, outer strike-point position and an example Langmuir probe I_{sat} signal (probe located at $R=0.71\text{cm}$). Radial extents of the full probe array are shown in (c).

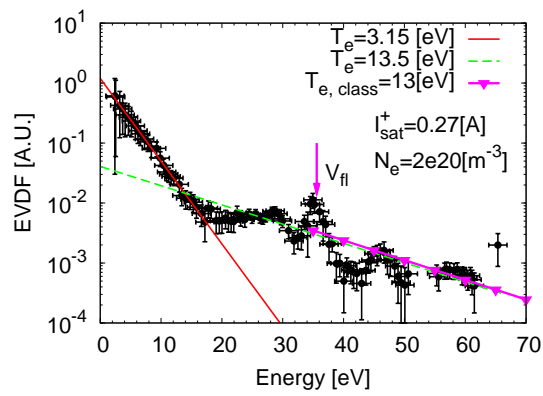


Figure 3: Plot showing derived electron velocity distribution function(EVDF) vs. energy. EVDF derived using kinetic interpretation of the I-V characteristic with best-fit values of a bi-modal distribution also shown. Electron temperature derived from conventional analysis of the I-V characteristic yields 13 eV.

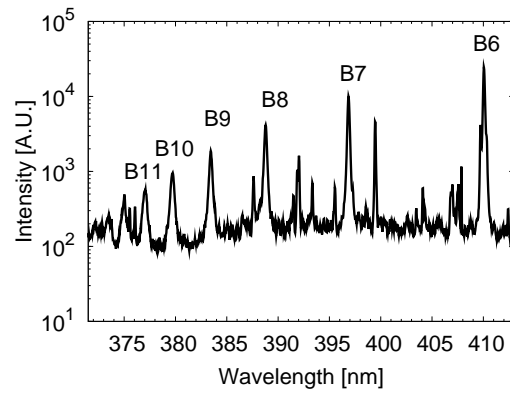


Figure 4: Plot of divertor emission between 370–415 nm located over the probe array used in this study. The Hydrogen Balmer lines 6–11 have been labeled.

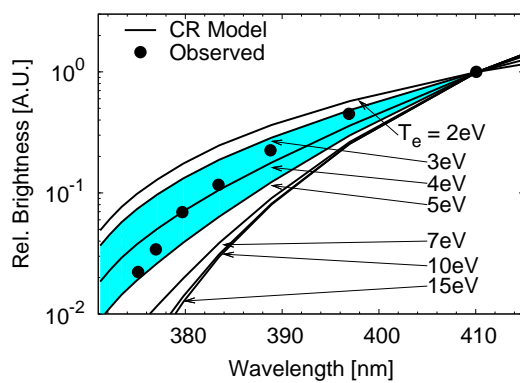


Figure 5: Plot of relative line intensities vs. wavelength for 10% neutral background density and a range of electron temperatures of the background plasma. All line intensities normalized to the Balmer-6 line at 410 nm. Region between 3–5 eV highlighted to indicate range of temperatures bounding experimental data.

List of Tables

- 1 Summary of Langmuir probe and spectroscopic analyses. “Bulk” values refer to those obtained from the kinetic probe interpretation method. 18

Table 1: Summary of Langmuir probe and spectroscopic analyses. “Bulk” values refer to those obtained from the kinetic probe interpretation method.

Quantity	Value	Quantity	Value
Classical n_e	$1.6 \times 10^{20} \text{ m}^{-3}$	Classical T_e	8.3 eV
Bulk n_e	$2.5 \times 10^{20} \text{ m}^{-3}$	Bulk T_e	3.4 eV
Broadening n_e	$3.6 \pm 1.5 \times 10^{20} \text{ m}^{-3}$	CRM T_e	3–5 eV

The Princeton Plasma Physics Laboratory is operated
by Princeton University under contract
with the U.S. Department of Energy.

Information Services
Princeton Plasma Physics Laboratory
P.O. Box 451
Princeton, NJ 08543

Phone: 609-243-2245
Fax: 609-243-2751
e-mail: pppl_info@pppl.gov
Internet Address: <http://www.pppl.gov>